

Enhanced thermal performance of closed-cell rigid Polyurethane (PU) foam panels using phase change materials (PCMs)

Adham M. Mohammed¹, Amira Elnokaly², Abdel Monteieb M. Aly¹ and Mohamed H. Mahmoud¹

¹Department of Architecture, Faculty of Engineering, University of Assuit, Egypt

² School of Architecture and the Built Environment, University of Lincoln, UK

Abstract

The consequences of extreme energy consumption are seen both in the energy and environmental crisis. Subsequently, researchers are attempting to find methods to address this issue. Building envelopes and insulation materials are elements that can effectively influence consumption through their passive effect on thermal comfort levels. Strategies pertaining to this that rely on both, advanced and traditional materials, have been able to show good potential. However, the technical complexity of using such strategies can be impeded from the perspective of developing countries. With the aim of creating effective low-cost feasible insulations through using methods of minimal intricacies, the potentials of simple amalgamation of materials is empirically investigated in this study. In this context, closed-cell rigid Polyurethane (PU) foam is used as a base to hold phase change materials (PCMs) to create two PU/PCM panels, of different PCM content. The thermal performance of the panels is experimentally examined and compared, with hot-arid climates prevailing in developing countries in mind. Results revealed that panels containing PCMs were able to perform more effectively in comparison with regular PU foam panels, and, that increasing the amount of PCM has also shown to be advantageous in this regard.

Keywords: Simple amalgamation; Thermal insulation; Phase change materials; Thermal performance; Heat peak temperature; Heat peak shift.

Abbreviations

PCM	Phase change material
PU panel	Polyurethane panel
PU/PCM150 panel	Panel containing PU foam and 150ml of PCM
PU/PCM300 panel	Panel containing PU foam and 300ml of PCM
HPT	Heat peak temperature
μ	Weighted mean heat peak time

1. Introduction

In hot-arid climate regions, it is estimated that up to 70-80% of total energy consumption is used through active cooling systems [1]. Consequently, reducing the reliance on those will have a drastic impact on energy consumption. An optimized envelope design can improve the thermal performance through passive solar techniques [2-4]. Many passive attempts to limit the effect of exterior heat on building interior temperatures have been successful [5,6], thus, increasing thermal comfort in hot climates and reducing strain on HVAC systems [7-10]. Traditional methods have also shown good results, in some cases comparable to modern passive thermal control methods [2,11,12]. Namely, multiple investigations seem to agree on the merits of using PCMs as part of building walls [13-16]. Wang et al. [17] used a 5 cm thick layer of paraffin wax to show that it is possible to reduce heat gain through exterior walls and reduce indoor temperatures from 34.7 to 32 °C. Where, Biswas et al. [18] showed a possible 32% reduction of wall-related cooling electricity consumption through numerically simulating a

thinner layer of PCMs as thermal insulation. Similarly, Xie et al. [19] support this by examining the behaviour of PCMs exposed to hot and cold airflow when in contact with building exteriors. Another empirical study reports that a reduction in energy consumption of 48.5% and 44% in both summer and winter could be achieved via PCM being placed inside holes in bricks [20]. Other studies have come to similar conclusions that confirm the potential benefits of using PCMs [21-25]. Also, PCMs infused into wallboards through various techniques have shown to provide significant reductions in gained heat and thermal energy [26-30]. Similar advantageous attributes can be made via incorporating PCM in concrete which is used for both structural and thermal purposes [31-36]. This method can also be utilized so as to combine PCM with other materials such as plaster, gypsum and mortar [37-44]. Yet, more prominently, micro-encapsulation is observed to be most promising, which allows for PCM particles to be encased in the form encased segments of a Nano-scale size. Thus, allowing PCM to be impregnated into other materials to gain superior characteristics [32,45-50]. The advantages of adopting techniques such as these presented earlier are influential with regards to actively reducing energy consumption, despite the variation in estimating the degree of possible energy savings ranging from 20% to 50.8%. [51-58]. Despite the aforementioned promising attributes in the literature presented above, critically examining the methods used to utilize PCMs, it can be seen that techniques that are of high complexity are required, such as micro-encapsulation for instance. Where

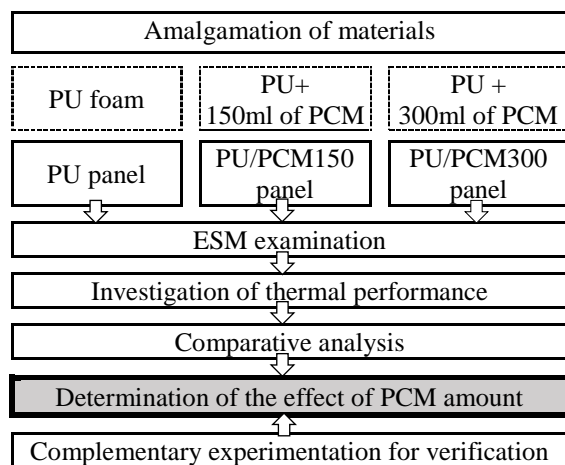
Received:5 July, 2020, Accepted:12 July, 2020

such techniques may be feasible for some, other locations around the world can find such intricate techniques hampering, thus, impeding the adoption of PCM-based insulations. In an attempt to further promote the usage of PCMs, a simplified method of encapsulating PCMs are explored as a novel approach of utilising the beneficial properties of PCM rather than the common complex methods presented in literature. Hence, PU foam is used to house the PCMs, to create low-cost feasible thermal insulation panels. Yet, the focus of the present study is to evaluate the effect of the amount of PCM encapsulated within the PU foam structure. The significance of this is that it highlights the capabilities of PCMs as a thermal insulator and shows the expected potential if the simplified methods of PCM incorporation are used to effectively enhance the performance of commercially-available insulation such as PU foam. Such panels being able to effectively perform better than the PU foam panels can further promote the use of the simplified method in areas of the world where high-tech incorporation methods, such as micro-encapsulation, can be impeding.

2. Materials and method of amalgamation

In this study, PU foam and PCMs are amalgamated into panels with two different amounts of PCM. The thermal performance of the panels is investigated to determine the effect of the different quantities of PCM. Table 1 shows the methodology and sequence followed to achieve this, and the details of the process is elucidated in the following.

Table 1: Methodology and sequence of investigation.



Closed-cell rigid Polyurethane (PU) foam is used as a form of encapsulation of the PCM and a commercially-available type of PU foam (CFSTTM 2-part liquid foam) is investigated, shown in Figure 1(A). The foam mixture entailed of two compounds, namely, Part A which is a Polymeric MDI and part

B which contains Poly-etherols, flame-retardant, Silicone, Catalyst and Blowing agents, to be mixed with almost equal volume ratio (1:1.06), as is instructed by the provider. The components of this type of PU foam are expected to expand to 25 times the initial volume of the PU mixture. The PCM used in the context of this study was Paraffin wax with a melting temperature of 43°C. Figure 1(B) shows blocks of the mentioned PCMs being melted for the creation of one of the panels. This specific type of PCM is used as its melting temperature is suitable for the prevailing weather conditions in the middle east reign. A wooden mold with dimensions of 20*20*1 cm (inner dimensions) was created for the purpose of creating the tested panels. The mold is fixed on a non-stick fibre re-enforced plastic sheet to avoid the PU mixture from adhering to the work surface. Tape was used to fix the mold in place and avoid any possible leakage from the mold. After the investigated PU mixture is poured into the mold, a tile is placed on top of the mold with 5 kg of weights. Figure 1(C). shows the mentioned PU panel set-up.

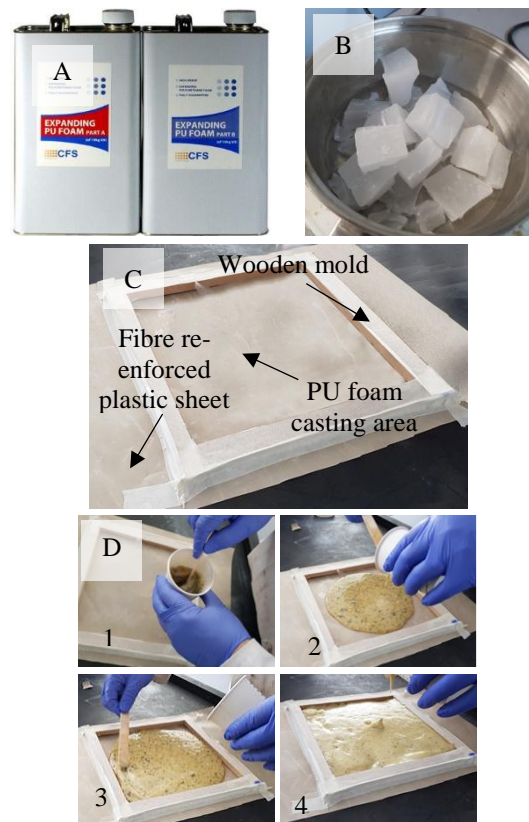


Figure 1: (A) CFSTTM 2-part liquid foam (part A&B). (B) PCM blocks. (C) Mold used to create PU panel, placed on a fibre re-enforced plastic sheet and fixed with tape to prevent leakage. (D) Creation of PU foams through mixing materials, placing mix inside casting are, spreading materials and expansion of materials.

To create a typical test panel, the components are mixed then are poured into the secured mold. The components are spread so as to fill the entire area of

the mold. The mentioned mixture begins to expand immediately after being placed within the mold. Hence, the upper restraint (tile with weights) is placed immediately on the mold. Figure 1(D) shows an example of the mentioned process for the creation of one of the examined panels. The mixture begins to exhibit initial solidification within 5 minutes of being cast into the mold. However, the upper restraint is removed after around 60 minutes of casting to ensure the complete solidification is attained. To investigate the performance of PU panels enhanced with PCMs three panels are created. A PU foam panel is created, used as a reference, and a PU panel containing an amount of 150ml of PCM, referred to as the PU/PCM150 panel. Also, a PU panel containing 300 ml of PCM is created to investigate the effect of increasing the amount of PCM, referred to as the PU/PCM300 panel. All the created panels were of identical dimensions and of a volume of 400 cm³.

In a previous study, optimal methods to amalgamate PCMs into the structure of PU foam have been investigated. This was carried out to investigate simplified incorporation methods that are of low intricacies. Through the mentioned study, it was determined that the optimal method of incorporation is to cool the PCM to -15°C, for a duration of several hours, so that the complete solidification of the PCM was ensured. This allowed the PCM to be of a brittle nature. The PCM was then ground multiple times, using a regular kitchen blender, till the point it is of a powder-like consistency, that is homogeneous in size. The granules of the PCM were measured to be 0.10 - 0.25 mm in diameter. PCM granules can be seen in Figure 2(A). SEM images of the amalgams were then taken to examine their micro-structure. This showed that the PCM granules have been homogeneously dispersed in the PU foam without any PCM accumulations. Figure 2(B) shows the location of PCM granules dispersed in a sample of the panel. Additionally, the PCM granules were found to have been sufficiently engulfed with PU cells, except for some superficial granules. According to several SEM measurements, such as shown in Figure 2(C), the granule sizes of PCM inside the panel were confirmed to range from 0.10 to 0.25mm. The intermediate distance between the mentioned granules was found to range from 0.25 to 1.2 mm. Also, as seen in Figure 2(D), no chemical reactions have been observed between the PCM granules and the PU foam as a distinct separation can be seen between the two materials. It is worthy to also mention that another viable method of amalgamation was the PCMs being mixed with component B of the PU foam through strenuous stirring, using a magnetic stirrer at a high RPM for a duration of 30 minutes until the mixture was homogeneous. The next step was to add component A of the PU foam. It is important to mention, however, that the

mentioned earlier method seems to result in leakages of the PCM in cases where large quantities of PCMs are used, such as in the PU/PCM300 panel. Figure 2(E) show the PU/PCM150 panel after being removed from the mold. The PU/PCM300 panel is shown in Figure 2(F).

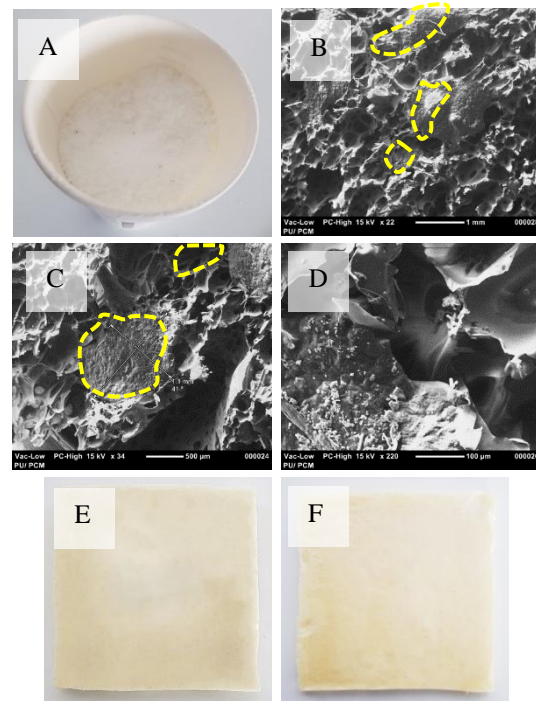


Figure 2: (A) Frozen PCM ground into a powder-like form. (B) SEM image showing the location/dispersion of PCM granules in a sample of PU/PCM panel. (C) Size of a single PCM granule. (D) No chemical reactions between the PCM and the PU foam have been observed. (E) PU/PCM150. (F) PU/PCM300.

3. Investigation of the thermal performance

As the aim of the created panels is to serve as thermal insulation, investigating their thermal performance inside a space in which they may be used would be imperative. The tested panel is placed between the two controlled environments. Then, a pre-set heat variation is applied to one of the sides of the panel. As the temperature would vary on the side of the panel as a result of this variation, the other side would gradually be thermally influenced in correspondence to this variation. Through measuring the air temperature on both sides and comparing them, the thermal performance could be assessed. Figure 3(A) below shows a schematic representation describing the position of the tested panel concerning the controlled environments applied.

3.1. Experimental set-up

To test created panels, a suitable container is created to house the tested panels. The container used for this experiment was created using sheets of MDF wood that were cut using an Epilog Fusion

M2™ Laser cutter and engraver for precise cutting/dimensions and to eliminate possible heat-leakage. The container is constructed of a frame of MDF wood with a thickness of 10 mm. The inner dimensions were 20 * 24 cm so as to accommodate the panels (20 * 20 cm) and a void for possible expansion (4 cm). The wooden frame was coated with four layers of sealant to eliminate the possibility of air leakage. Both sides of the frame were covered with sheets of Plexi-glass of 2mm thickness. The container after assembly is shown in Figure 3(B). As mentioned earlier, two different environments are required to influence the tested panels. A box-like confinement is made of 18 mm thick sheets of medium density fibre wood (MDF) that were cut and assembled to the required dimensions. The inner dimensions of the confinement were 20cm*20cm*35cm, with a platform to hold the panels at the front. The mentioned confinement was insulated using wood-fibre sheets (Diall™ Fibre wood underlay) with a thickness of 5mm. The sheets were obtained from a local provider and are sold originally as 50 * 70 cm sheets for floor thermal underlay. Seven layers of the fibre-wood were added, in total 35 mm of insulation. The total thickness of the confinement's wall at this point is 53mm. Figure 3(C) shows the confinement after final assembly including fibre-wood insulation. To subject the panel under investigation to environment-like conditions, the panels and the insulated confinement were placed inside an environmental chamber. The environmental chamber used was a Panasonic™ versatile environmental test chamber model MLR-352 as shown in Figure 3(D&E). Also, to monitor the change in air temperature of both side of the panel throughout the duration of the experiment, two HOBO® MX Temp/RH Data Loggers model-(MX1101) were used, shown in Figure 3(F). The data loggers have a range of -20° to 70°C with an accuracy of ±0.21°C and are capable of logging up to one reading per second. Control and setup of the data loggers can be done through an iOS or Android™ device through a Bluetooth® connection. Logged data is also downloaded through a wireless connection.

3.2. Empirical Investigation and procedures

The panel under testing is placed in the panel holder, mentioned earlier. Then, the holder is in turn placed in its designated location in the confinement, which is previously kept, open, at room temperature for a duration of at least 24 hours. The entire set-up at this point is placed in the chamber, which is sealed. Data loggers are placed, one inside the confinement prior to placing the panel holder and inside the chamber. Both loggers are placed so as to be at a distance of 5 cm from the corresponding surface of the tested panel. Figure 3(G) shows a test panel placed into a holding panel, in this case, the PU

panel. Figure 3(H) shows the entire assembly of the panel inside the confinement, placed into the environmental chamber.

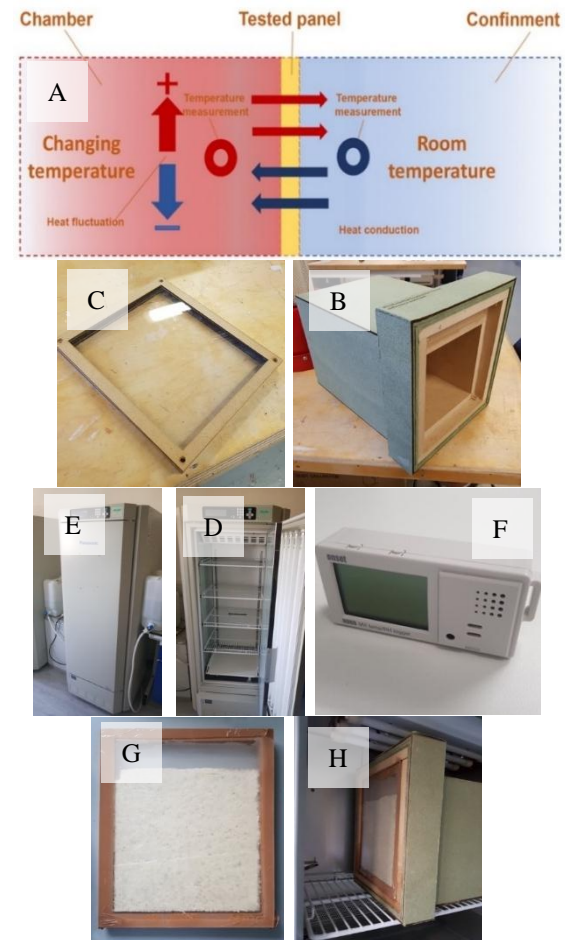


Figure 3: (A) Schematic representation of the experimental procedures carried out on the tested panels (Authors' own). (B) The encapsulation container after assembly. (C) The Box-like confinement with the platform end to hold the PCM encapsulation container. (D) Exterior of environmental chamber, (E) Interior of chamber, (F) HOBO® MX Temp/RH Data Logger model-(MX1101). (G) PU panel inserted into the holding panel. (H) Assembly of the tested panel and the confinement, inside the environmental chamber.

Three profiles were set-up. Namely, profile A, which represents heat condition similar to this of a natural hot-weathered location. Also, profile B, representing exposure to a long duration of relatively high heat and profile C, representing exposure to several short duration of heat bursts. Details of the mentioned heat profiles are presented in Table 2. It should be noted that the actual applied heat temperatures inside the chamber differ from the pre-set values due to the abilities of the chamber and accumulation of heat, Table 2 shows the actual applied heat inside the environmental chamber, measured using data loggers. A representation of the applied heat profiles can be seen in the context of

Figure 4 below. To further show the validity of the empirical set-up, several repetitions of the experimental process using a different type of loggers, were carried out. A number of nine repetitions was conducted for each panel under exposure to each profile, totalling twenty-seven repetitions per panel. For this purpose, nine additional data loggers were utilised to further accuracy and to eliminate possible error due failure in the apparatus. The obtained data from the verification experiments is then compared to this obtained from the main experimental process, thus an assessment of the accuracy and validity of the process is obtained. It is worthy to note that, in terms of accuracy of measurements, the maximum variation in measurements for the PU panel was $\pm 0.015^{\circ}\text{C}$, for the PU/PCM150 panel was $\pm 0.130^{\circ}\text{C}$ and for the PU/PCM300 panel was $\pm 0.030^{\circ}\text{C}$. The mentioned minimal variations allow the procedure to be considered verified and of high accuracy.

Table 2: Measured applied heat and pre-set heat.

Profile	Total duration (hours)	Min. temp. ($^{\circ}\text{C}$)	Max. temp. ($^{\circ}\text{C}$)	Cycle Cycles	Cycle duration (hours)
A	24	14	50	1	12
B	12	35	50	1	6
C	3	35	50	3	1

3.3. Results

Based on the literature [17,18,20,59–62], certain aspects of insulation describe its thermal performance. The data obtained through the previously mentioned process sheds light on some of these aspects. The heat peak temperature (HPT) describes the highest temperature that occurred during a certain thermal test, whether outside or inside the confinement. Hence, the HPT reduction can be calculated based on the difference between the HPT of the applied temperature and this measured inside the confinement at the presence of the tested panel. As it describes the ability of a panel to retain a portion of the exerted heat, the shift in the HPT is calculated in the form of the weighted mean heat peak (μ) shift, which considers the duration at which the temperature continues for a duration of time. Equation 1 explains the method of calculating the weighted mean heat peak.

Equation 1: Calculation of weight mean heat peak.

$$\mu = \frac{\sum_{i=1}^n (x_i * w_i)}{\sum_{i=1}^n w_i}$$

Where,

μ is the weighted mean.

X are the observed values, in this case, the temperature readings.

W are the weights for values, in this case, the logged duration for each temperature.

n is the number of readings for each curve.

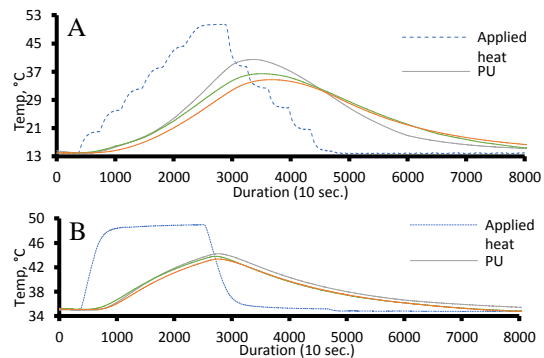
The calculation of the (μ) shift for the tested samples is calculated as:

$$\mu \text{ shift} = \mu \text{ of tested panel} - \mu \text{ of applied heat}$$

The measurement obtained through the testing mentioned earlier have been used to calculate the values described in the previous sections for each panel, under all heat profiles. Table 3 presents the mentioned calculations. It may be worthy to note that visual examination was carried out on all of the tested panel after exposure to several cycles of heat. This revealed that no leakage had occurred in any of the panels. Furthermore, with the exception of the PU panel, no panel had shown shrinkage of a notable extent. A comparison between the measured temperatures, inside and outside the confinement, for all profile can be seen in the plots shown in Figure 4. The applied heat is also shown.

Table 3: Thermal performance of the tested panels.

Profile	Max. temp. ($^{\circ}\text{C}$)	Min. temp. ($^{\circ}\text{C}$)	HPT red. ($^{\circ}\text{C}$)	HPT shift (Min.)	μ (Min.)	μ Shift (Min.)
PU panel						
A	40.64	14.0	9.95	8.07	64.86	22.86
B	44.20	35.0	4.77	4.75	54.08	24.12
C	41.30	35.0	6.97	7.82	47.90	19.91
PU/PCM150 panel						
A	36.42	14.0	14.17	11.23	68.40	26.40
B	43.79	35.0	5.18	3.68	54.19	24.23
C	40.90	35.0	7.37	8.70	49.19	21.20
PU/PCM300 panel						
A	34.75	14.0	15.84	13.21	72.74	30.74
B	43.34	35.0	5.63	4.81	54.30	24.35
C	38.41	35.0	9.86	6.17	50.06	22.06



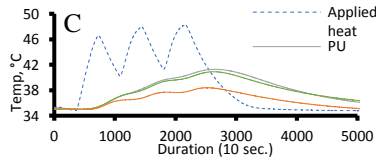


Figure 4: Temperature plots for the tested panels. (A) Profile A. (B) Profile B. (C) Profile C.

3.4. Analysis and discussion

Through comparing the HPT reduction that is measured in the panels with this in the PU panel, it can be seen that all of the amalgams have caused a temperature reduction that is greater than this caused by the PU panel. That is to say that the amalgam panels perform better in terms of thermal insulation than the commercially-available PU foam. Figure 5(A, B & C) present a plot showing a comparison between the tested panels in terms of heat reduction inside the confinement, for all profiles. The figure clearly shows that the presence of PCM within the structure of the PU foam was advantageous. In the case of the PU/PCM150 panel, in profile A, the HPT was reduced by a 4.22°C compared to the PU panel. Then, the increased amount of PCM in the PU/PCM300 panel resulted in an additional increase of 1.67°C, in the same heat profile. Furthermore, profile B and C show correlation to this in terms of HPT, with the PU/PCM300 panel showing least HPT. It is worthy to note that the amplitude of reduction in HPT is seen to be less in profile B than A, and less in C than B. This can be expected as a result of the reduced duration of exposure to heat, which impedes the amount of heat absorbed within the mass of the PCM. A comparison between the tested panel with regards to the shift in μ is presented in Figure 5 (F). Similar to the HPT reduction, it is apparent that the shift in μ is increased as the amount of used PCM is increased. This strongly correlates with literature that shows that PCM can retain an amount of heat due to its latent heat properties, hence, the greater the amount used the more heat which would be stored in the PCM. Such heat is later released, causing an increase in the μ shift. Likewise, the shift in μ is seen to decrease as the duration of exposure decreases, in profile B then C, which is consistent with previous findings.

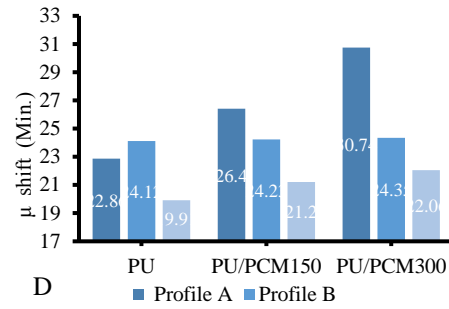
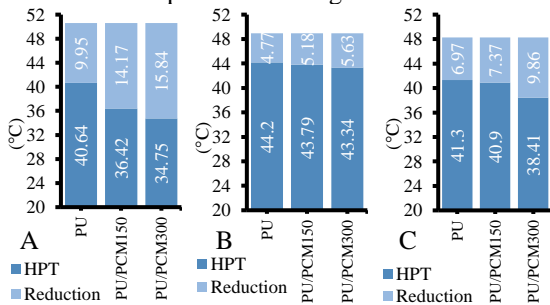


Figure 5: (A) HPT and HPT reduction for profile A. (B) for profile B. (C) for profile C. (D) Shift in μ .

The area encompassed under a (time-temperature) curve can represent the thermal energy that is exerted. For instance, the area under the curve of the applied heat temperature can signify the thermal energy exerted by the chamber. Similarly, the area under the curves of the measured temperatures inside the confinement signifies the gained thermal energy through the panel. Hence, as seen in Figure 6, the amount of energy that has been shifted and re-distributed along the duration of the testing process can be calculated. For all profiles, the thermal energy in the chamber and in the confinement is calculated using the method of trapezoidal approximation, a method commonly used for such calculations [63–67]. In this case, the mentioned method has provided precise calculations due to the high number of readings that were taken at a 10-second interval between each measurement. For each test, the shared area under both curves, applied heat and measured temperatures as seen in Figure 6, is calculated as:

$$\text{Shared energy} = \text{area under } (P1 \text{ to } P2) + (P2 \text{ to } P3)$$

Where,

P1 is the starting point of experiment.

P2 is the point at which applied heat and measured temperatures curves intersect.

P3 the end point of the applied heat curve.

Hence, the amount of energy that has displaced (shifted) from the chamber and into the confinement, referred to as "shifted energy", is calculated, as a percentage of the total energy of the applied heat, as:

$$\frac{(\text{Area Under applied heat} - \text{shared energy (area)})}{\text{Area Under curve of applied heat}} * 100$$

The shared energy affects the inside of the confinement, detected as energy inside the confinement. Yet in certain cases, some losses in the mentioned energy are observed to occur due to various factors. This loss, referred to as "Energy reduction", is calculated as:

$$\begin{aligned} \text{Energy reduction (\%)} &= \text{Shifted (delayed)energy (\%)} \\ &\quad - \text{Gained energy (\%)} \end{aligned}$$

Whereas, the gained energy that describes the energy received inside the confinement can be calculated as:

$$\frac{(\text{Area Under panel tem.} - \text{shared energy}(\text{area}))}{\text{Area Under curve of applied heat}} * 100$$

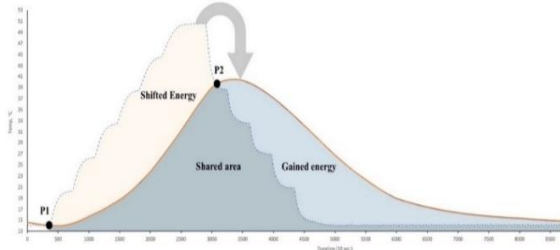


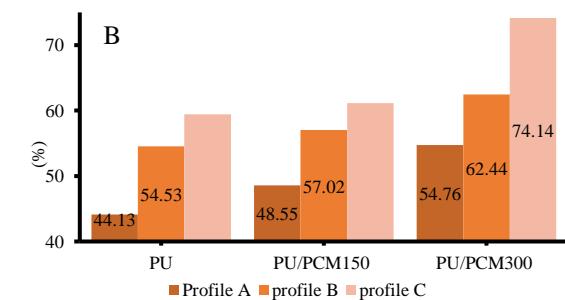
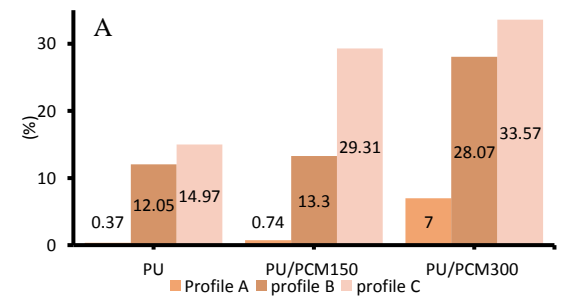
Figure 6: Example showing the areas calculated under a curve. The figure shows the shared area between the curves describing temperatures outside and inside the confinement. The shifted and gained energy are displayed.

The significance of calculating this is that it sheds light on the capability of the amalgams to retain an amount of thermal energy to be released at a more convenient time, such as cooler, night-time, thus allowing for other natural-cooling strategies such as natural ventilation to take effect. Table 4 shows the shifted and gained energies, as a percentage of the applied energy, for all the tested panel in all profiles. Also, the reduction in energy is presented. The degree to which the amount of energy is reduced is seen to be consistent with the reduction in HPT, as would be expected. Table 4(A) shows a comparison between the calculated energy reduction for all profiles of the tested panels. As is in the case of HPT reduction, the effect of the amount of PCM is clear. Comparing the PU, PU/PCM150 and PU/PCM300 panels, it is seen that greater amounts of PCM will result in more reduced energy. It is likely that when the applied heat reaches its lower temperatures, the stored thermal energy in the form of heat is partially dissipated. Thus, lower energy is observed in the confinement. It is also apparent that the amount of reduced energy is increased with reduced exposure durations, which is to be expected as, in this case, the reduced energy is not only as a result of PCM properties but also as a result of insufficient time for the applied heat to take effect. An example of the is the reduction in energy caused by the PU/PCM300 in profile C, of 33.57%, compared to this in profile A of 14.97%. The amount of thermal energy that has been absorbed by the panel and released into the confinement over a longer duration of time can be indicative of the amalgams capability to stabilize temperatures. This is represented by the shifted energy, which is presented as a percentage of the total applied energy in each profile. Table 4(B) shows a comparison between the shifted energy for all panels. It is observed that this is in correlation with the amounts

of reduced energy. Likewise, the PU/PCM300 is seen to provide the most shifted energy, with 72.14% in profile C, and the PU panel has provided the least. Similar correlation as previous, in terms of effect of heat duration, is apparent for the shifted energy.

Table 4: Energy shift and reduction for the control panels and (A) Plot of reduction in energy inside the confinement. (B) Plot of shifted energy.

Profile	Shifted energy (%)	Gained energy (%)	Energy reduction/ Gain (%)
PU panel			
A	44.13	43.76	0.37
B	54.53	48.30	12.05
C	59.42	44.45	14.97
PU/PCM150 panel			
A	48.55	47.81	0.74
B	57.02	41.32	13.3
C	61.12	31.81	29.31
PU/PCM300 panel			
A	54.76	47.76	7.0
B	62.44	34.37	28.07
C	74.14	40.58	33.57



4. Complementary thermal experimentation

To further investigate and validate the thermal performance of the created panels, other two set-ups were created. The first allows for samples of 20* 50* 10 mm of the created panels to be exposed to direct heat from a hot-plate. As heat flows through the sample, a thermal camera monitors the temperatures and the pace of heat flow. The mentioned set-up is seen in Figure 7(A). The second set-up includes a furnace at which the sample is heated to 60 °C, as shown in Figure 7(B). Then, the samples are allowed

to cool as they are monitored by a thermal the detect the maximum and minimum inner temperatures, as seen in Figure 7(C). In both set-ups, precautions are taken to allow for a precise comparison between the tested samples such as the use of wind-shields and controlling AC temperatures to ensure a constant ambient temperature. Thermal images were able to shed light on the thermal properties of the materials. Such properties showed that the increase in PCM content is seen to be able to reduce the pace at which heat is able to flow. Furthermore, it is seen to result in increasing the ability to retain heat for longer durations, possibly due to PCM thermal storage capabilities, which is consistent with previous findings.

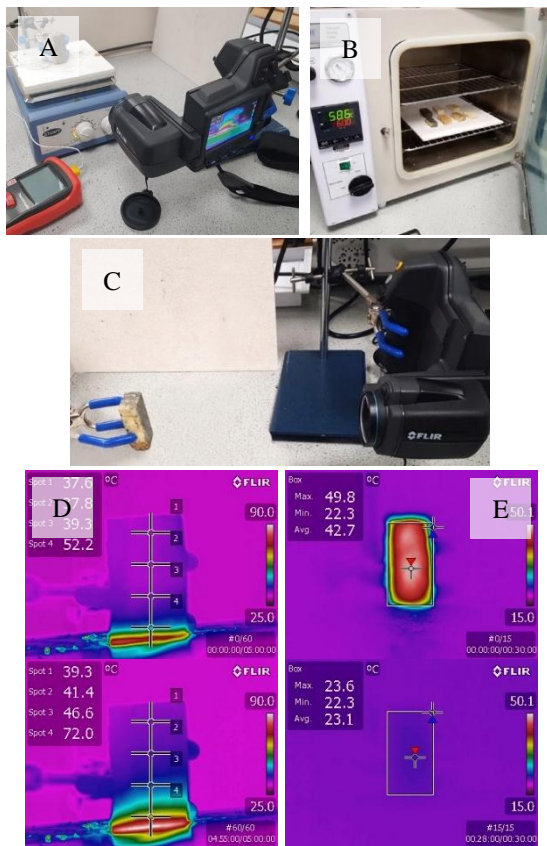


Figure 7: (A) First experimental set-up. (B) Samples placed in oven for heating to 60°C. (C) Second experimental set-up. (D) Examples of thermal images from the first experimental set-up. (E) Examples of thermal images from the second experimental set-up.

5. Conclusions

Through the process of testing the thermal performance of the panels created via amalgamating PU foam and PCM, several conclusions are found. The intricate methods to impregnate or encapsulate PCMs and other materials are not necessary for the creation of PCM-based insulations. Also, the closed-cell nature of PU foam can provide good shielding for the amalgamated material. The thermal

performance of the PCM-panels was superior than this of the PU foam panel, indicating that the simplified method can result in thermal insulations that are of a performance superseding this of commercial-available insulations. Thus, reducing production costs and further promote using insulations in developing areas of the world. Increasing the amount of PCM content within the created panels has considerable effect on the thermal performance. The PU/PCM300 panel performed noticeably better than the PU/PCM150 panel in almost all aspects, such as reduction in peak temperatures, (μ) shift and gained energy reduction. Hence, it can be inferred that increasing PCM amount has a favourable influence on PU foam insulations. In cases of long exposure to heat, the thermal performance is seen to be more efficient than cases of shorted exposure. This is to be expected as a result of the PCM fully or partially melting, which sheds light on the importance of selecting a suitable PCM based on the weather patterns in the location where it is to be utilised, which is in agreement with previous studies.

6. Acknowledgements

The authors wish to acknowledge the Egyptian ministry of higher education for funding the work presented in this article as part of a joint-supervision PhD programme. The authors also extend their thanks and appreciation to Dr. Nicholas Tucker from the University of Lincoln for providing assistance and facilitating the use of equipment and resources essential for the creation of this work.

7. References

- [1] Koch-Nielsen H 2013 Stay Cool : A Design Guide for the Built Environment in Hot Climates (Routledge)
- [2] Ayoub M and Elseragy A 2018 Parameterization of traditional domed-roofs insulation in hot-arid climates in Aswan, Egypt Energy & Environment 29 109–30
- [3] Elnokaly A and Elseragy A 2007 What impedes the development of renewable energy technology in Egypt MCEET 2007 Sustainable Energy: Technologies, Materials and Environmental Issues (Cairo, Egypt: MCEET, Cairo, Egypt)
- [4] Fahmy M, Mahdy M M and Nikolopoulou M 2014 Prediction of future energy consumption reduction using GRC envelope optimization for residential buildings in Egypt Energy and Buildings 70 186–93
- [5] Feist W, Schnieders J, Dorer V and Haas A 2005 Re-inventing air heating: Convenient and comfortable within the frame of the Passive House concept Energy & Buildings 11 1186–203
- [6] Holmes M J and Hacker J N 2007 Climate change, thermal comfort and energy: Meeting the design challenges of the 21st century Energy and Buildings 39 802–14
- [7] Burillo D, Chester M V, Pincetl S, Fournier E D and Reyna J 2019 Forecasting peak electricity demand for Los Angeles considering higher air temperatures due to climate change Applied Energy 236 1–9
- [8] Jovanović S, Savić S, Bojić M, Djordjević Z and Nikolić D 2015 The impact of the mean daily air temperature change on electricity consumption Energy 88 604–9
- [9] Özbalt T G, Sezer A and Yıldız Y 2012 Models for Prediction of Daily Mean Indoor Temperature and Relative

- Humidity: Education Building in Izmir, Turkey Indoor and Built Environment 21 772–81
- [10] Zhang S, Cheng Y, Fang Z, Huan C and Lin Z 2017 Optimization of room air temperature in stratum-ventilated rooms for both thermal comfort and energy saving Applied Energy 204 420–31
- [11] Elnokaly A, Ayoub M and Elseragy A 2019 Parametric investigation of traditional vaulted roofs in hot-arid climates Renewable Energy 138 250–62
- [12] Elseragy A and Elnokaly A 2007 Assessment criteria for form environmental performance of building envelope in hot arid climates pp 156–62
- [13] Arıcı M, Bilgin F, Nižetić S and Karabay H 2020 PCM integrated to external building walls: An optimization study on maximum activation of latent heat Applied Thermal Engineering 165 114560
- [14] Khan R J, Bhuiyan Md Z H and Ahmed D H 2020 Investigation of heat transfer of a building wall in the presence of phase change material (PCM) Energy and Built Environment 1 199–206
- [15] Rathore P K S and Shukla S K 2019 Potential of macroencapsulated PCM for thermal energy storage in buildings: A comprehensive review Construction and Building Materials 225 723–44
- [16] Yang Y, Wu W, Fu S and Zhang H 2020 Study of a novel ceramicsite-based shape-stabilized composite phase change material (PCM) for energy conservation in buildings Construction and Building Materials 246 118479
- [17] Wang Q, Wu R, Wu Y and Zhao C Y 2018 Parametric analysis of using PCM walls for heating loads reduction Energy and Buildings 172 328–36
- [18] Biswas K, Shukla Y, Desjarlais A and Rawal R 2018 Thermal characterization of full-scale PCM products and numerical simulations, including hysteresis, to evaluate energy impacts in an envelope application Applied Thermal Engineering 138 501–12
- [19] Xie J, Wang W, Sang P and Liu J 2018 Experimental and numerical study of thermal performance of the PCM wall with solar radiation Construction and Building Materials 177 443–56
- [20] Dabiri S, Mehrpooya M and Nezhad E G 2018 Latent and sensible heat analysis of PCM incorporated in a brick for cold and hot climatic conditions, utilizing computational fluid dynamics Energy 159 160–71
- [21] Cao V D, Pilehvar S, Salas-Bringas C, Szczotok A M, Bui T Q, Carmona M, Rodriguez J F and Kjøniksen A-L 2019 Thermal analysis of geopolymers concrete walls containing microencapsulated phase change materials for building applications Solar Energy 178 295–307
- [22] Dardir M, Roccamena L, Mankibi M E and Haghightat F 2020 Performance analysis of an improved PCM-to-air heat exchanger for building envelope applications – An experimental study Solar Energy 199 704–20
- [23] de Gracia A 2019 Dynamic building envelope with PCM for cooling purposes – Proof of concept Applied Energy 235 1245–53
- [24] Klimeš L, Charvát P, Mastani Joybari M, Zálešák M, Haghightat F, Panchabikesan K, El Mankibi M and Yuan Y 2020 Computer modelling and experimental investigation of phase change hysteresis of PCMs: The state-of-the-art review Applied Energy 263 114572
- [25] Saxena R, Rakshit D and Kaushik S C 2020 Experimental assessment of Phase Change Material (PCM) embedded bricks for passive conditioning in buildings Renewable Energy 149 587–99
- [26] Gnanachelvam S, Ariyanayagam A and Mahendran M 2019 Fire resistance of light gauge steel framed wall systems lined with PCM-plasterboards Fire Safety Journal 108 102838
- [27] Jeong S-G, Wi S, Chang S J, Lee J and Kim S 2019 An experimental study on applying organic PCMs to gypsum-cement board for improving thermal performance of buildings in different climates Energy and Buildings 190 183–94
- [28] Li C, Yu H and Song Y 2019 Experimental investigation of thermal performance of microencapsulated PCM-contained wallboard by two measurement modes Energy and Buildings 184 34–43
- [29] Park J H, Kang Y, Lee J, Wi S, Chang J D and Kim S 2019 Analysis of walls of functional gypsum board added with porous material and phase change material to improve hygrothermal performance Energy and Buildings 183 803–16
- [30] Wang H, Lu W, Wu Z and Zhang G 2020 Parametric analysis of applying PCM wallboards for energy saving in high-rise lightweight buildings in Shanghai Renewable Energy 145 52–64
- [31] Arivazhagan R, Arun Prakash S, Kumaran P, Sankar S, Loganathan G B and Arivarasan A 2020 Performance analysis of concrete block integrated with PCM for thermal management Materials Today: Proceedings 22 370–4
- [32] Pomianowski M and Jensen R L 2020 Heat storage in concrete deck with nano- and micro-encapsulated PCM Smart Nanoconcretes and Cement-Based Materials Micro and Nano Technologies ed M S Liew, P Nguyen-Tri, T A Nguyen and S Kakooei (Elsevier) pp 313–31
- [33] Qu Y, Chen J, Liu L, Xu T, Wu H and Zhou X 2020 Study on properties of phase change foam concrete block mixed with paraffin / fumed silica composite phase change material Renewable Energy 150 1127–35
- [34] Uthaichotirat P, Sukontasukkul P, Jitsangiam P, Suksiripattanapong C, Sata V and Chindaprasirt P 2020 Thermal and sound properties of concrete mixed with high porous aggregates from manufacturing waste impregnated with phase change material Journal of Building Engineering 29 101111
- [35] Vinayaka Ram V, Singhal R and Parameshwaran R 2020 Energy efficient pumpable cement concrete with nanomaterials embedded PCM for passive cooling application in buildings Materials Today: Proceedings
- [36] Yu N, Chen C, Mahkamov K, Han F, Zhao C, Lin J, Jiang L and Li Y 2020 Selection of a phase change material and its thickness for application in walls of buildings for solar-assisted steam curing of precast concrete Renewable Energy 150 808–20
- [37] Costa J A C, Martinelli A E, do Nascimento R M and Mendes A M 2020 Microstructural design and thermal characterization of composite diatomite-vermiculite paraffin-based form-stable PCM for cementitious mortars Construction and Building Materials 232 117167
- [38] Cunha S, Silva M and Aguiar J 2020 Behavior of cementitious mortars with direct incorporation of non-encapsulated phase change material after severe temperature exposure Construction and Building Materials 230 117011
- [39] Frigione M, Lettieri M, Sarcinella A and Barroso de Aguiar J 2020 Sustainable polymer-based Phase Change Materials for energy efficiency in buildings and their application in aerial lime mortars Construction and Building Materials 231 117149
- [40] Guo J, Jiang Y, Wang Y and Zou B 2020 Thermal storage and thermal management properties of a novel ventilated mortar block integrated with phase change material for floor heating: an experimental study Energy Conversion and Management 205 112288
- [41] Abden M J, Tao Z, Pan Z, George L and Wuhrer R 2020 Inclusion of methyl stearate/diatomite composite in gypsum board ceiling for building energy conservation Applied Energy 259 114113
- [42] Lee J, Wi S, Yun B Y, Yang S, Park J H and Kim S 2019 Development and evaluation of gypsum/shape-stabilization phase change materials using large-capacity vacuum impregnator for thermal energy storage Applied Energy 241 278–90
- [43] Wi S, Yang S, Lee J, Chang S J and Kim S 2019 Dynamic heat transfer and thermal performance evaluation of PCM-doped hybrid hollow plaster panels for buildings Journal of Hazardous Materials 374 428–36

- [44] Mekaddem N, Ali S B, Fois M and Hannachi A 2019 Paraffin/ Expanded Perlite/Plaster as Thermal Energy Storage Composite Energy Procedia 157 1118–29
- [45] Muthya Goud V, Vaisakh V, Joseph M and Sajith V 2020 An experimental investigation on the evaporation of polystyrene encapsulated phase change composite material based nanofluids Applied Thermal Engineering 168 114862
- [46] Singh Rathore P K, Shukla S K and Gupta N K 2020 Potential of microencapsulated PCM for energy savings in buildings: A critical review Sustainable Cities and Society 53 101884
- [47] Praveen B, Suresh S and Pethurajan V 2019 Heat transfer performance of graphene nano-platelets laden micro-encapsulated PCM with polymer shell for thermal energy storage based heat sink Applied Thermal Engineering 156 237–49
- [48] Cabeza L F, Navarro L, Pisello A L, Olivieri L, Bartolomé C, Sánchez J, Álvarez S and Tenorio J A 2019 Behaviour of a concrete wall containing micro-encapsulated PCM after a decade of its construction Solar Energy
- [49] Praveen B and Suresh S 2019 Thermal performance of micro-encapsulated PCM with LMA thermal percolation in TES based heat sink application Energy Conversion and Management 185 75–86
- [50] Agresti F, Fedele L, Rossi S, Cabaleiro D, Bobbo S, Ischia G and Barison S 2019 Nano-encapsulated PCM emulsions prepared by a solvent-assisted method for solar applications Solar Energy Materials and Solar Cells 194 268–75
- [51] Pop O G, Fehete Tutunaru L, Bode F, Abrudan A C and Balan M C 2018 Energy efficiency of PCM integrated in fresh air cooling systems in different climatic conditions Applied Energy 212 976–96
- [52] Ghahramani Zarajabad O and Ahmadi R 2018 Employment of finned PCM container in a household refrigerator as a cold thermal energy storage system Thermal Science and Engineering Progress 7 115–24
- [53] Bista S, Hosseini S E, Owens E and Phillips G 2018 Performance improvement and energy consumption reduction in refrigeration systems using phase change material (PCM) Applied Thermal Engineering 142 723–35
- [54] Wijesuriya S, Tabares-Velasco P C, Biswas K and Heim D 2020 Empirical validation and comparison of PCM modeling algorithms commonly used in building energy and hygrothermal software Building and Environment 173 106750
- [55] Yun B Y, Park J H, Yang S, Wi S and Kim S 2020 Integrated analysis of the energy and economic efficiency of PCM as an indoor decoration element: Application to an apartment building Solar Energy 196 437–47
- [56] Dardir M, Panchabikesan K, Haghghat F, El Mankibi M and Yuan Y 2019 Opportunities and challenges of PCM-to-air heat exchangers (PAHXs) for building free cooling applications—A comprehensive review Journal of Energy Storage 22 157–75
- [57] Chen X, Zhang Q, Zhai Z J and Ma X 2019 Potential of ventilation systems with thermal energy storage using PCMs applied to air conditioned buildings Renewable Energy 138 39–53
- [58] Mourid A, El Alami M and Kuznik F 2018 Experimental investigation on thermal behavior and reduction of energy consumption in a real scale building by using phase change materials on its envelope Sustainable Cities and Society 41 35–43
- [59] Li Z X, Al-Rashed A, Rostamzadeh M, Kalbasi R, Shahsavari A and Afrand M 2019 Heat transfer reduction in buildings by embedding phase change material in multi-layer walls: Effects of repositioning, thermophysical properties and thickness of PCM Energy Conversion and Management 195 43–56
- [60] Ryms M and Klugmann-Radziemska E 2019 Possibilities and benefits of a new method of modifying conventional building materials with phase-change materials (PCMs) Construction and Building Materials 211 1013–24
- [61] Zondag H A, de Boer R, Smeding S F and van der Kamp J 2018 Performance analysis of industrial PCM heat storage lab prototype Journal of Energy Storage 18 402–13
- [62] Piselli C, Castaldo V L and Pisello A L 2018 How to enhance thermal energy storage effect of PCM in roofs with varying solar reflectance: Experimental and numerical assessment of a new roof system for passive cooling in different climate conditions Solar Energy
- [63] Yeh C-T 2017 Existence of interval, triangular, and trapezoidal approximations of fuzzy numbers under a general condition Fuzzy Sets and Systems 310 1–13
- [64] Ban A, Coroianu L and Grzegorzewski P 2011 Trapezoidal approximation and aggregation Fuzzy Sets and Systems 177 45–59
- [65] Yeh C-T 2008 Trapezoidal and triangular approximations preserving the expected interval Fuzzy Sets and Systems 159 1345–53
- [66] Coroianu L 2011 Best Lipschitz constant of the trapezoidal approximation operator preserving the expected interval Fuzzy Sets and Systems 165 81–97
- [67] Grzegorzewski P and Pasternak-Winiarska K 2014 Natural trapezoidal approximations of fuzzy numbers Fuzzy Sets and Systems 250 90–109

الأداء الحرارى لرغوة البولى يوريثين (PU) الصلبة ذات الخلايا المغلقة المدعمة بالمواد متغيرة الطور (PCMs)

ملخص البحث:

للإستخدام المفرط للطاقة تأثيرا ملحوظا على مشكلتى البيئة و نفاذ الطاقة. ومن هذا المنطلق، يحاول العديد من الباحثون إيجاد الحلول المناسبة لهذا الأمر. وتعد أغلفة المباني ومواد العزل الحرارى من العناصر الهامة والتي قد يكون لها تأثير ملحوظ للحد من الإستخدام المفرط للطاقة. ويكون ذلك من خلال تأثيرها الإيجابى على درجات الحرارة داخل المباني. وتعتبر الإستراتيجيات التى تأخذ ذلك بعين الإعتبار من الإستراتيجيات التى أبدت نجاحا كبيرا، والتي إعتمدت بشكل كبير على كل من المواد المتطورة والتقليدية على حد السواء. إلا أنه، وعلى الرغم من ذلك، فإن التعقيدات التكنولوجية اللازمة لتطبيق تلك الإستراتيجيات قد تعتبر عائقا وخاصة أمام الدل النامية والتي قد لا تمتلك المقدره على إستخدام هذه الأساليب. من هذا المنطلق فإن هذه الدراسة تهتم ببحث و بإستخدام أسلوب الدمج المبسط للمواد، بهدف تكوين مواد صالحة للعزل الحرارى تتمتع بتكلفة منخفضة وسهولة التصنيع. وفى هذا السياق، يتم إستخدام رغوة البولى يوريثين (PU) الصلبة مغلقة الخلايا كقاعدة لتحميل كمية من المواد متغيرة الطور (PCMs) وذلك لتكوين ألواح عازلة للحرارة. وقد تم اختبار أداء العزل الحرارى للألواح التى تم تصنيعها، وذلك مع وضع المناخ الجاف الحار نصب الإعتبار حتى تحاكي الإختبارات الظروف المناخية السائدة فى منطقة الشرف الأوسط. وقد أوضحت الإختبارات المجرأه فاعلية الألواح المصنعة من حيث الأداء الحرارى مقارنة بأداء ألواح البولى يوريثين العادية. كما أوضحت إمكانية تحسين الأداء الحرارى عن طريق زيادة كمية المواد متغيرة الطور.

الكلمات المرجعية: أسلوب الدمج المبسط، العزل الحرارى، المواد متغيرة الطور، الأداء الحرارى، درجة الحرارة القصوى، الترحيل الحرارى.